

Article

Development of a Novel Electrochemical Biosensor Based on Organized Mesoporous Carbon and Laccase for the Detection of Serotonin in Food Supplements

Dorin Dăscălescu and Constantin Apetrei * 

Department of Chemistry, Physics and Environment, Faculty of Sciences and Environment, “Dunărea de Jos” University of Galați, 47 Domnească Street, 800008 Galați, Romania

* Correspondence: apetreic@ugal.ro; Tel.: +40-727-580-914

Abstract: Serotonin is a biogenic amine that has multiple roles in the human body and is mainly known as the happiness hormone. A new laccase (Lac)-based biosensor has been developed for the qualitative and quantitative determination of serotonin in three dietary supplements from three different manufacturers. The enzyme was immobilized on an organized mesoporous carbon-modified carbon screen-printed electrode (OMC-SPE) by the drop-and-dry method, the active surface being pretreated with glutaraldehyde. With the new biosensor, serotonin was selectively detected from different solutions. Square-wave voltammetry was the technique used for the quantitative determination of serotonin, obtaining a detection limit value of 316 nM and a quantification limit value of 948 nM in the linearity range of 0.1–1.2 μM . The *pH* for the determinations was 5.2; at this value, the biocatalytic activity of the laccase was optimal. At the same time, the electrochemical performance of the OMC-SPE/Lac biosensor was compared with that of the unmodified sensor, a performance that highlighted the superiority of the biosensor and the very important role of the enzyme in electro-detection. The results obtained from the quantitative determination of serotonin by square-wave voltammetry were compared with those from the FTIR method, revealing a very good correlation between the results obtained by the two quantitative determination methods.

Keywords: serotonin; laccase; biosensor; square-wave voltammetry; food supplements



Citation: Dăscălescu, D.; Apetrei, C. Development of a Novel Electrochemical Biosensor Based on Organized Mesoporous Carbon and Laccase for the Detection of Serotonin in Food Supplements. *Chemosensors* **2022**, *10*, 365. <https://doi.org/10.3390/chemosensors10090365>

Academic Editor: Győző G. Láng

Received: 2 August 2022

Accepted: 9 September 2022

Published: 11 September 2022

Publisher's Note: MDPI stays neutral with regard to jurisdictional claims in published maps and institutional affiliations.



Copyright: © 2022 by the authors. Licensee MDPI, Basel, Switzerland. This article is an open access article distributed under the terms and conditions of the Creative Commons Attribution (CC BY) license (<https://creativecommons.org/licenses/by/4.0/>).

1. Introduction

Serotonin (5-hydroxytryptamine, 5-HT) is a biogenic amine found in biological systems, both as a neurotransmitter in the central nervous system and as a hormone in the peripheral nervous system and gastrointestinal tract. It is also a factor in platelet aggregation, being a component of platelets [1]. Serotonin is directly involved in the regulation of body temperature, sleep, sexual drive, and appetite. It also has a positive influence on well-being [2]. There are 10 mg of serotonin in the body, 2% of which is distributed in the central nervous system, and any disturbance of this level, either through an excess or a deficit, alters the body's balance, triggering a series of pathological conditions. More specifically, the concentrations of serotonin in the body, taking into account the distribution of this biogenic amine according to biological fluid samples, are below 0.0568 nM in the cerebrospinal fluid [3], about 0.27–1.49 nM in serum, and 0.3–1.65 nM in urine [4–6].

Low serotonin levels are correlated with a number of conditions such as depression, schizophrenia, Parkinson's syndrome, obsessive–compulsive syndrome, cardiovascular disease, Alzheimer's disease, bipolar disorder, anxiety, and migraine [7,8], and high levels can trigger serotonin syndrome, an excessive activity of nerve cells manifested by hypertension, hyperthermia, seizures, and rhabdomyolysis. In addition, exacerbated amounts of serotonin occur in carcinoid syndrome (a tumor of the small intestine, appendix, and colon) and can affect liver regeneration [9].

Due to the accelerated pace of development in the food and pharmaceutical industries during the last decades and based on the increasing interest of companies in the mentioned industries in accurately determining the composition of foods and dietary supplements to detect allergens or various harmful compounds, it has been found that some foods contain serotonin in appreciable amounts, including avocados, pineapples, bananas, plums, peanuts, tomatoes, and eggplants [10]. Serotonin is found in large amounts in *Mucuna pruriens*, along with flavonoids, tannins, levodopa, alkaloids, terpenes, and phenolic compounds [11,12].

To date, serotonin has been determined in food and biological fluids by numerous techniques, such as high-performance liquid chromatography [13–16], electrophoresis [17–20], spectrophotometry [21], fluorescence [22–24], chemiluminescence [16,25], etc.

Although highly accurate, these techniques involve long working times, complex preliminary steps for sample preparation, and sometimes the use of toxic substances. All these impediments do not allow real-time analysis. As complementary methods to classical analytical techniques, a number of electrochemical serotonin detection methods have been developed in recent years using sensors and biosensors, which are viable alternatives, as these devices have a number of advantages, namely, simple handling, low costs, short working times, and high sensitivity and selectivity. Among the most widely used electrochemical techniques are cyclic voltammetry, square-wave voltammetry, and differential pulse voltammetry [26–29]. Each method has specific features. For example, cyclic voltammetry provides information about the processes taking place at the electrode surface, while square-wave voltammetry is characterized by good selectivity and the absence of background currents, as in differential pulse voltammetry.

Numerous electrodes modified with nanomaterials of different types have been used to monitor the electrochemical behavior and to perform qualitative and quantitative analyses of human biological fluids or plant products containing serotonin. These include multiwalled carbon nanotubes and gold nanoparticles [30], multiwalled carbon nanotubes with magnetic particles, graphene oxide electrodes reduced with silver nanoparticles [31], graphene oxide reduced with silver selenide [32], and polypyrrole and ferrocene oxide-modified carbon screen-printed electrodes [33]. Composite nanomaterials have also been used with good results in electrochemical detection techniques, including the one with Ag, polypyrrole, and Cu nanoparticles [34], that with SnO₂-SnS₂ [35], and those based on CeO nanofibers, Au, and RuO₂ [36]. The selectivity and sensitivity of the sensors listed above were influenced on the one hand by the type of carbon electrode used and on the other hand by the properties of the nanomaterial chosen to modify the respective electrode.

Recent research in electrochemistry has focused on the development of biosensors, which have superior properties to electrodes modified with nanocomposite materials in terms of sensitivity and selectivity. The literature refers to various biosensors, such as one with nanodiamond and gold nanoparticles anchored in a casein biofilm [37], a carbon paste electrode with horseradish peroxidase [38], and a platinum and laccase electrode [39]. These biosensors have been used to detect serotonin in synthetic urine and blood samples from rats [38,40].

Having proven the analytical performance of enzymes in the detection of serotonin in various biological and food samples, the use of laccase was proposed for the fabrication of a new biosensor, taking into account the electrocatalytic properties of this enzyme.

Laccase enables direct electron transfer (DET), which occurs between the active redox enzyme and the electrode surface and produces electronic coupling between the redox protein and the electrode. The redox enzyme acts as an electrocatalyst, facilitating electron transfer between the electrode and the molecular substrate without involving a mediator in the process. Accordingly, biosensors capable of direct electron transfer have higher selectivity because they are less exposed to interference. A small number of enzymes are able to interact directly with the electrode, catalyzing the related enzymatic reaction, e.g., laccase, in a way that could favor DET [41].

Laccase consists of four copper atoms: T1, T2, and two T3 atoms [42–46]. The T1 site of Cu is located near the surface of the enzyme in the hydrophobic fold where the enzyme substrate attaches. The oxygen-binding site is represented by the trinuclear T2/T3 cluster, which is 13 Å apart from the T1 site [47].

The present study aims to detect serotonin in *Mucuna pruriens*-based dietary supplements by voltammetric methods using a newly developed biosensor. At the same time, the present study aims to compare the performance of the OMC-SPE organized mesoporous carbon screen-printed electrode with the laccase-modified biosensor (OMC-SPE/Lac) in terms of active surface areas, surface coverage with the electroactive species, and detection and quantification limits.

The novelty of the study lies in the fact that we used a newly constructed biosensor based on laccase to detect serotonin from the plant *Mucuna pruriens*. As far as we know, the literature has not reported sensors and biosensors for the detection of levodopa from this plant. Knowing that, in the brain, it is metabolized into dopamine, which is recognized for its effects on motivation and attention, we found it useful to confirm the presence of serotonin in *Mucuna pruriens*. The detection of serotonin in *Mucuna pruriens* could make the product recommended in the treatment of depression as well as Parkinson's syndrome.

2. Materials and Methods

2.1. Materials, Reagents, and Solutions

Monosodium phosphate, phosphoric acid, potassium bromide, and catechol were purchased from Sigma-Aldrich (St. Louis, MO, USA). Phosphate buffer solution (PBS) was prepared by dissolving NaH_2PO_4 in ultrapure water obtained via the Milli-Q Millipore system (Bedford, MA, USA), and the *pH* of this solution was adjusted with phosphoric acid and checked with the Inolab *pH* 7310 *pH* meter (WTW, Weilheim, Germany). Preliminary tests were performed in 10^{-1} M phosphate buffer solution (PBS) at *pH* 5.2 and in a 10^{-3} M catechol solution with 10^{-1} M PBS.

Serotonin of analytical purity was supplied by Sigma-Aldrich. A stock solution of 10^{-3} M concentration was obtained by dissolving serotonin in 10^{-1} M (*pH* 5.2) PBS. Laccase extracted from *Trametes versicolor*, concentration 0.9 U/mg, was purchased from Sigma-Aldrich. A laccase solution with a concentration of $50 \mu\text{g}\cdot\mu\text{L}^{-1}$ was prepared by dissolving the enzyme powders, previously weighed, in 1 mL of 10^{-1} M (*pH* 5.2) PBS. A similar concentration of the laccase solution was also reported in another paper [48]. Ultrasonication was used for homogenization. The obtained solution was clear and slightly yellowish in color [43]. The laccase stock solution was stored at -4°C when not in use. The solutions of the real samples were obtained by dissolving different amounts of powder from the capsules in 50 mL of 10^{-1} M *pH* 5.2 phosphate buffer solution. The dissolution operation was followed by ultrasonication (Elmasonic Carl Roth GmbH, Karlsruhe, Germany) for homogenization and filtration to remove insoluble compounds from the solutions to be analyzed.

The samples analyzed by the FTIR spectrometric method were prepared using potassium bromide of analytical purity for both standard and real samples. The amino acids phenylalanine, tyrosine, and tryptophan were purchased from Sigma-Aldrich and were used in the interference studies.

2.2. Electrodes and Equipment

The sensors were electrochemically characterized with a model 263 A EG&G potentiostat/galvanostat (Princeton Applied Research, Oak Ridge, TN, USA) equipped with an electrochemical cell consisting of three electrodes. The working electrode was the sensor or the biosensor, the reference electrode was Ag/AgCl (3M KCl), and the counter electrode was a platinum wire. The potential of Ag/AgCl (3 M KCl) versus a normal hydrogen electrode is 0.197 V. All the electrode potentials have been reported versus an Ag/AgCl (3 M KCl) reference electrode. A mesoporous organized carbon-based screen-

printed electrode (OMC-SPE) and a laccase-modified mesoporous organized carbon-based screen-printed electrode (OMC-SPE/Lac) were the working electrodes.

The OMC-SPE electrode was purchased from Metrohm-DropSens (Llanera, Spain). Experimental data were recorded and processed with ECHEM software. The Bruker ALPHA FT-IR spectrometer (BrukerOptik GmbH, Ettlingen, Germany) with OPUS software (BrukerOptik GmbH, Ettlingen, Germany) was used for the FTIR analysis of commercial products.

2.3. Biosensor Preparation

In the first step, the OMC-SPE electrode was functionalized using glutaraldehyde by placing that electrode over a 2% glutaraldehyde pot for 1 min. In the second step, 10 μL of the laccase enzyme solution was deposited on the surface of the OMC-SPE sensor by the drop-and-dry technique after previously obtaining the 50 $\mu\text{g}\cdot\mu\text{L}^{-1}$ laccase enzyme solution by dissolving this enzyme in 10^{-1} M PBS (pH 5.2). Cross-linking with glutaraldehyde allows the formation of covalent bonds between the aldehyde group of glutaraldehyde and the free amino groups of the laccase enzyme. Enzyme cross-linking generally involves the free ϵ -amino groups of the lysine residues, as the lysine residues do not affect the catalytic site, leaving the conformation of the enzyme unchanged while preserving the biological activity of the enzyme [49].

After fabrication, the OMC-SPE/Lac biosensor was kept at room temperature before drying in a desiccator for 60 min and then stored at 4 $^{\circ}\text{C}$ until use.

2.4. Real Samples Analyzed

The *Mucuna pruriens* products selected for analysis were purchased from health food stores. *Mucuna* DOPA came from Haya Labs, *Mucuna pruriens* Organic Powder was produced by Bio Raw Foods, and *Mucuna pruriens* L-Dopa was manufactured by Haya Labs. These supplements induce a state of well-being in the human body, increase resistance to physical and mental stress, relieve tremor in Parkinson's syndrome, and regulate libido, according to the manufacturer's claims [50].

2.5. Methods of Analysis

Cyclic voltammetry in the potential range between -0.4 and $+1.3$ V was used to stabilize the electrochemical signal in 0.1 M PBS solution (pH 5.2), applying a scan rate of $0.1 \text{ V}\cdot\text{s}^{-1}$. For electrochemical determinations with the two sensors in 10^{-3} M catechol solution and in 10^{-3} M serotonin solution, the potential range between -0.4 V and $+0.7$ V was chosen at scanning rates between 0.1 and $1 \text{ V}\cdot\text{s}^{-1}$. The electrochemical parameters used in square-wave voltammetry were optimized by successive trials and adjusted according to the observed peak current, resulting in a frequency of 15 Hz, a pulse height of 90 mV, and a scan increment of 7 mV.

Spectrometric measurements were performed in the range of $4000\text{--}500 \text{ cm}^{-1}$ with an FTIR-ATR spectrometer (attenuated total reflectance sampling mode). The ZnSe crystal was cleaned after each determination with ultrapure water and then with isopropanol. Potassium bromide was mixed with the samples taken in the work. A 0.1 g/g serotonin standard sample was used for quantitative determinations. All FTIR determinations were performed in triplicate. The absorbance at the wavenumber related to the vibration of the $-\text{NH}_2$ group at 3285 cm^{-1} [51] was used for quantitative determinations.

3. Results

3.1. FTIR Characterization of Sensor and Biosensor

FTIR spectra were recorded (Figure 1) for the pure compound used for laccase crosslinking, glutaraldehyde, and for the OMC-SPE electrode to identify the peaks that could undergo changes following enzyme immobilization.

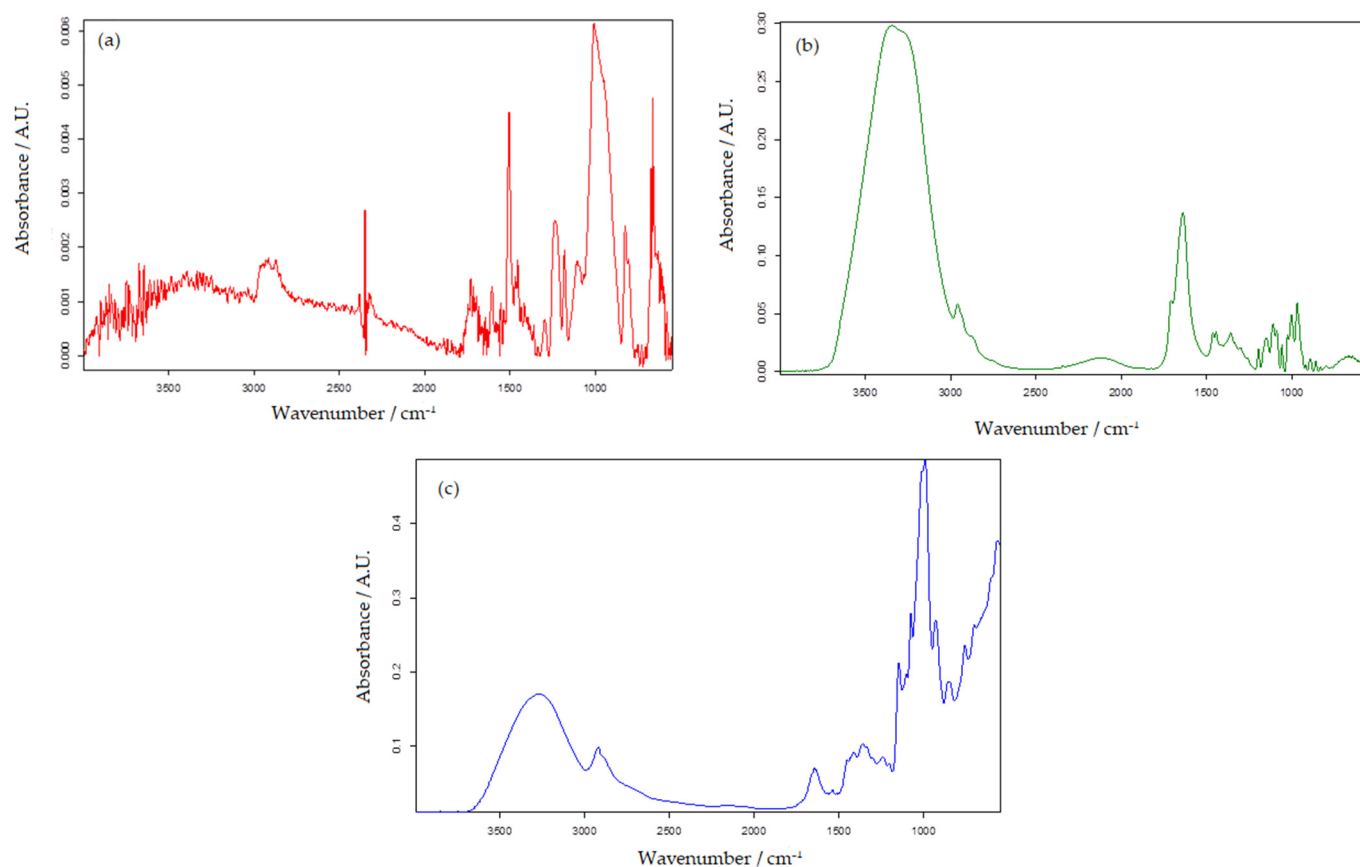


Figure 1. FTIR analysis of OMC-SPE (a), glutaraldehyde (25% aqueous solution) (b), and OMC-SPE/Lac (c).

In the case of the OMC-SPE (Figure 1a) spectrum, the bands present between 3000 and 3700 cm⁻¹ were attributed to the stretching vibration of the –OH present in the hydroxyl or carboxyl group [52]. The bands present in the range of 3000–2850 cm⁻¹, corresponding to the stretching vibrations of –CH [53], suggest the presence of aliphatic groups in the ordered mesoporous carbon structure.

Broad intense bands extended in the range of 1000 to 1500 cm⁻¹ were attributed to stretching vibrations of C–O in ester or ether and –OH bending vibrations in hydroxyl [54].

FTIR analysis allows the identification of proteins and polypeptides with nine specific IR absorption bands, such as amides A, B, and I through VII, of which bands I and II exhibit distinct vibrational bands to a high degree in the basic protein structure [55–57].

The amide I band of the protein is the most sensitive area, corresponding to the IR spectrum in the range of 1700–1600 cm⁻¹. This band appears as a result of stretching vibrations of the C=O groups in the peptide bonds. The amide I band reflects the secondary structure of the protein, while the amide II band indicates the in-plane folding of the –NH–group. Taking these properties into account, it follows that amide band I is more sensitive than amide band II in FTIR spectral analysis [55,58].

The FTIR spectra of OMC-SPE/Lac (Figure 1) show prominent peaks at 3388, 1655, 1584, 1425, and 1454 cm⁻¹. The broad band at 3388 cm⁻¹ shows the presence of NH stretching, and OH stretching of hydrogen intermolecular interactions [59] present between laccase and glutaraldehyde. The peak at 2917 cm⁻¹ (Figure 1c) shows the presence of aliphatic C–H stretching vibrations, also evident in Figure 1a. The peak corresponding to the amide (II) in the laccase structure is at 1584 cm⁻¹ (Figure 1c).

The peaks at 1360, 1240, 851, and 758 cm⁻¹ show the presence of CH₂ bending, O–H in-plane bending, N–H wobble, and O–H out-of-plane bending [59].

When two or more substances are mixed, physical versus chemical interactions are reflected by changes in characteristic spectral peaks. After the cross-linking, changes were observed, such as in the spectra and the slight shift of the peaks due to the hydrogen bonds between OH and NH^{3+} from laccase and the OH group from glutaraldehyde. Moreover, crosslinking between the enzyme and glutaraldehyde was confirmed by the formation of a new C=N band at approximately 1584 cm^{-1} and the shift of the band from 1638 cm^{-1} (Figure 1b) to 1644 cm^{-1} (Figure 1c), which suggests the CONH peptide bond [60].

From the obtained results, it can be appreciated that Lac remains unchanged after immobilization by cross-linking on the screen-printed electrode.

3.2. Preliminary Studies

The two electrodes, OMC-SPE and OMC-SPE/Lac, were first characterized by cyclic voltammetry in a 0.1 M PBS solution (pH 5.2) at a scan rate of $0.1\text{ V}\cdot\text{s}^{-1}$. Studies on the optimization of electrochemical parameters led to the observation that the potential range between -0.4 and $+1.4\text{ V}$ of the electrochemical signal of the sensors is stable.

In the cyclic voltammograms no oxido-reduction peaks are observed, demonstrating that no electro-active species are present in the reference solution and no impurities are present on the electrode surface to influence the electrochemical signals (Figure 2).

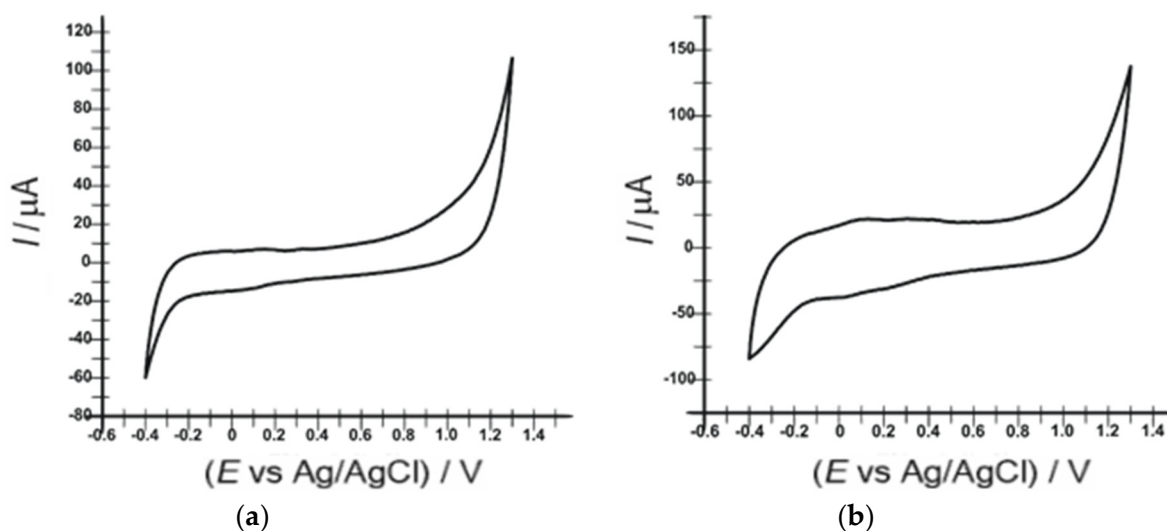


Figure 2. Cyclic voltammograms of (a) OMC-SPE and (b) OMC-SPE/Lac immersed in 0.1 M PBS (pH 5.2) at a $0.1\text{ V}\cdot\text{s}^{-1}$ scan rate.

Considering that the oxidation of the electro-active species studied in this paper (catechol and serotonin) usually takes place at a lower potential [61,62], in the following experiments the potential range of -0.4 – $+0.8\text{ V}$ was used. In the second phase, the electrochemical behavior of the two sensors was followed in a 10^{-3} M catechol and 10^{-1} M PBS solution.

Figure 3 shows the cyclic voltammograms of the unmodified sensor and the biosensor immersed in 10^{-3} M catechol solution and 10^{-1} M PBS at a scan rate of $0.1\text{ V}\cdot\text{s}^{-1}$.

Table 1 shows the electrochemical parameters of the unmodified sensor and biosensor in the voltammograms in Figure 3.

The OMC-SPE/Lac biosensor showed higher values of anodic and cathodic peak intensities than the unmodified electrode. The findings indicate that the oxido-reduction process of catechol is facilitated by the presence of the enzyme on the biosensor surface. Therefore, laccase has an important biocatalytic effect, increasing the sensitivity of the biosensor compared to the sensor containing no enzyme.

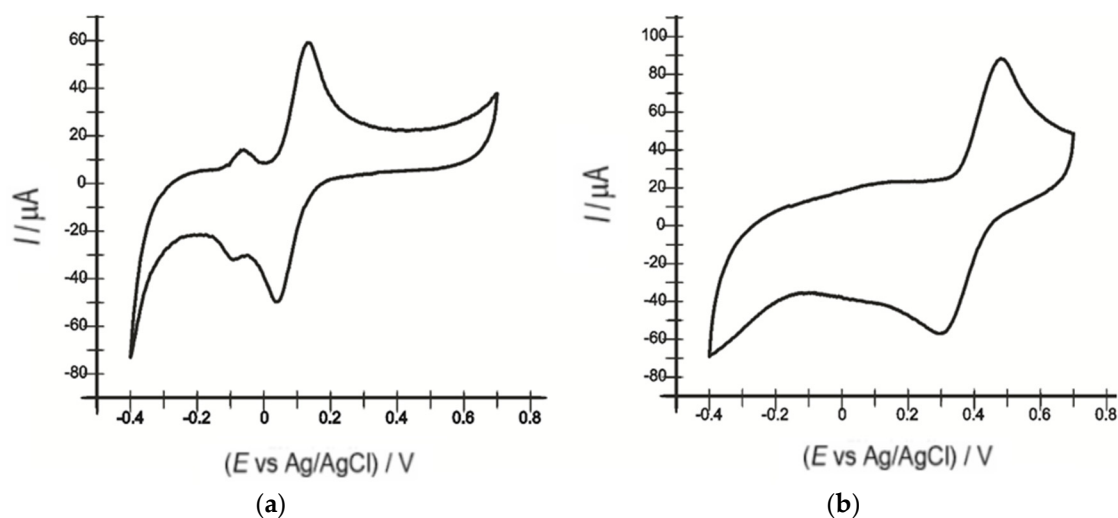


Figure 3. Cyclic voltammograms recorded of (a) OMC-SPE and (b) OMC-SPE/Lac immersed in a 10^{-3} M catechol solution and 0.1 M PBS at a $0.1 \text{ V}\cdot\text{s}^{-1}$ scan rate.

Table 1. Electrochemical parameters obtained by the two sensors after immersion in 10^{-3} M catechol and a 10^{-1} M PBS solution.

Sensor	I_a^1 (μA)	I_c^2 (μA)	I_c/I_a	E_{pa}^3 (V)	E_{pc}^4 (V)	$E_{1/2}^5$ (V)	ΔE^6 (V)
OMC-SPE	58.95	-49.34	0.83	0.135	0.105	0.170	0.130
OMC-SPE/Lac	88.08	-56.76	0.64	0.482	0.299	0.390	0.183

¹ Anodic peak current; ² cathodic peak current; ³ anodic peak potential; ⁴ cathodic peak potential; ⁵ half-wave potential $E_{1/2} = (E_{pa} + E_{pc})/2$; ⁶ $\Delta E = E_{pa} - E_{pc}$.

3.3. Determination of the Active Area of OMC-SPE and OMC-SPE/Lac

Cyclic voltammograms of the two sensors were recorded at scanning rates between $0.1 \text{ V}\cdot\text{s}^{-1}$ and $1 \text{ V}\cdot\text{s}^{-1}$ to determine the active areas of these two electrodes.

As the scanning rate increased, there was a slight shift in potential values towards lower potentials (cathode peak) and higher potentials (anode peak). An increase in the intensities of the cathode-related peaks with increasing scanning rates was also evident (Figure 4).

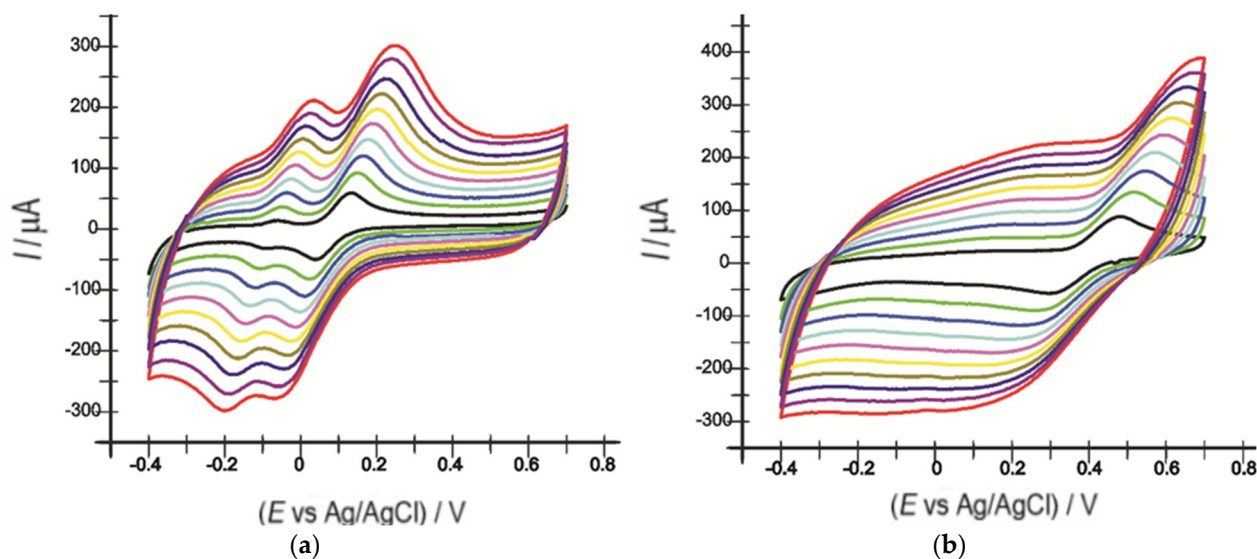


Figure 4. CVs of OMC-SPE (a) and OMC-SPE/Lac (b) in a 10^{-3} M catechol solution and 0.1 M PBS at different scanning rates (0.1, 0.2, 0.3, 0.4, 0.5, 0.6, 0.7, 0.8, 0.9, and $1.0 \text{ V}\cdot\text{s}^{-1}$).

By recording the CVs of the two electrodes, varying the scan rate between 0.1 and $1 \text{ V}\cdot\text{s}^{-1}$, a linearity between I_{pa} and the square root of the scan rate was revealed, with the equation of the fitting line being $I(A) = 0.0004 v^{1/2}(\text{V}\cdot\text{s}^{-1})^{1/2} - 6.26 \times 10^{-5}$ (Figure 5) and the coefficient of determination (R^2) being 0.9962 for the OMC-SPE/Lac biosensor.

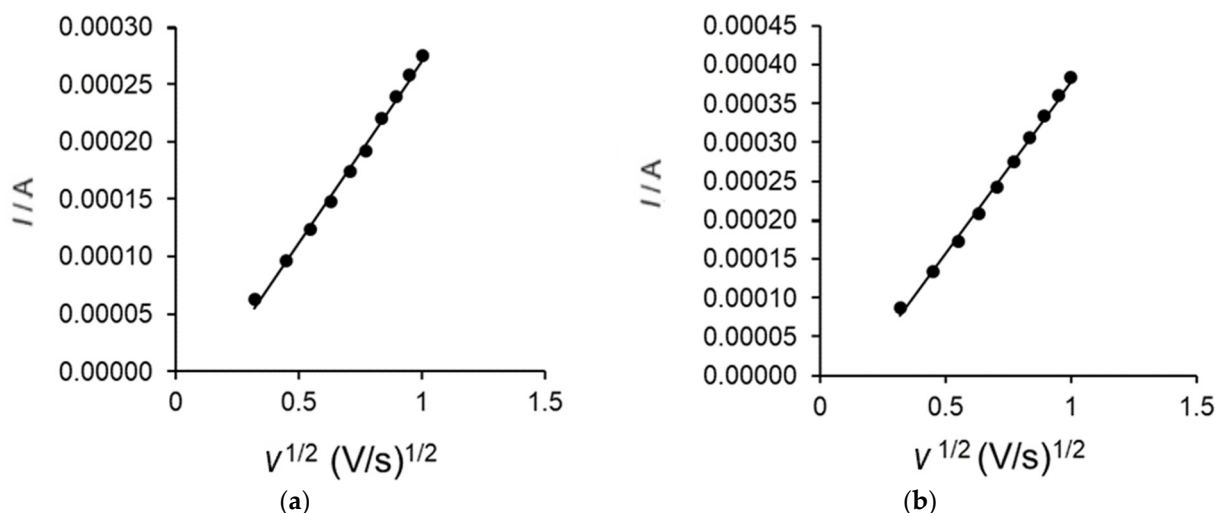


Figure 5. Linear dependence between anode current intensity and square root of scan rate for OMC-SPE (a) and OMC-SPE/Lac (b).

The values of the active surface areas of the two sensors are included in Table 2.

Table 2. Linear fit equation, R^2 , active surface area, and roughness factor of the two sensors.

Electrode	I_{pa} vs. $v^{1/2}$	R^2	A (cm^2)	Roughness Factor
OMC-SPE	I_{pa} (A) = $3.15 \times 10^{-4} v^{1/2}(\text{V}\cdot\text{s}^{-1})^{1/2} - 4.53 \times 10^{-5}$	0.9944	0.144	1.146
OMC-SPE/Lac	I_{pa} (A) = $4.40 \times 10^{-4} v^{1/2}(\text{V}\cdot\text{s}^{-1})^{1/2} - 6.26 \times 10^{-5}$	0.9962	0.201	1.600

Considering the obtained results, it was deduced that the process at the electrode surface is controlled by the diffusion of the active species. Therefore, the Randles–Sevcik equation was used to determine the active surface area of each sensor [63–65]:

$$I_{pa} = 268,600 \times n^{3/2} \times A \times D^{1/2} \times C \times v^{1/2}$$

where I_{pa} is the anode peak current (A), n is the number of electrons transferred in the redox process, A is the electrode area (cm^2), D is the diffusion coefficient ($\text{cm}^2\cdot\text{s}^{-1}$), C is the concentration ($\text{mol}\cdot\text{cm}^{-3}$), and v is the scan rate ($\text{V}\cdot\text{s}^{-1}$).

Taking into account the diffusion coefficient of catechol reported in the literature ($D = 8.5 \times 10^{-6} \text{ cm}^2\cdot\text{s}^{-1}$ [66]) and the linear regression equation of I_{pa} vs. $v^{1/2}$, the active surface areas of OMC-SPE and OMC-SPE/Lac were determined.

The values of these active surface areas are shown in Table 2.

In contrast to liquid electrodes (i.e., mercury), the surface of a solid electrode is not always smooth, and its real area exceeds the geometric one. In the case of modification with electrocatalytic nanomaterials (OMC for example) the active surface can be much larger than the geometric area and differs depending on the type of electrode.

Therefore, an important parameter is the roughness factor. It was calculated by the ratio between the real and the geometric surfaces of the electrodes.

It is important to know this ratio (its value should exceed 1) because all the obtained results are influenced by the active surface of the electrode and must be interpreted in relation to it [67].

The OMC-SPE/Lac biosensor has both a larger active surface area and a higher roughness factor than OMC-SPE, which means that it possesses more active centers than the unmodified sensor. The results are comparable to those of other electrodes reported in the literature [68].

3.4. Voltammetric Responses of the Unmodified Sensor and Biosensor in Serotonin Solutions

In the qualitative and quantitative determination of serotonin using the two sensors, OMC-SPE and OMC-SPE/Lac, the oxido-reduction process was investigated in a 10^{-3} M serotonin solution (PBS 10^{-1} M, $pH = 5.2$). The electrochemical signal stabilized in the potential range between -0.4 and $+0.7$ V after recording three cycles.

Figure 6 shows the cyclic voltammograms of the sensor and biosensor in a 10^{-3} M serotonin solution and 10^{-1} M PBS ($pH 5.2$) at $0.1 \text{ V}\cdot\text{s}^{-1}$.

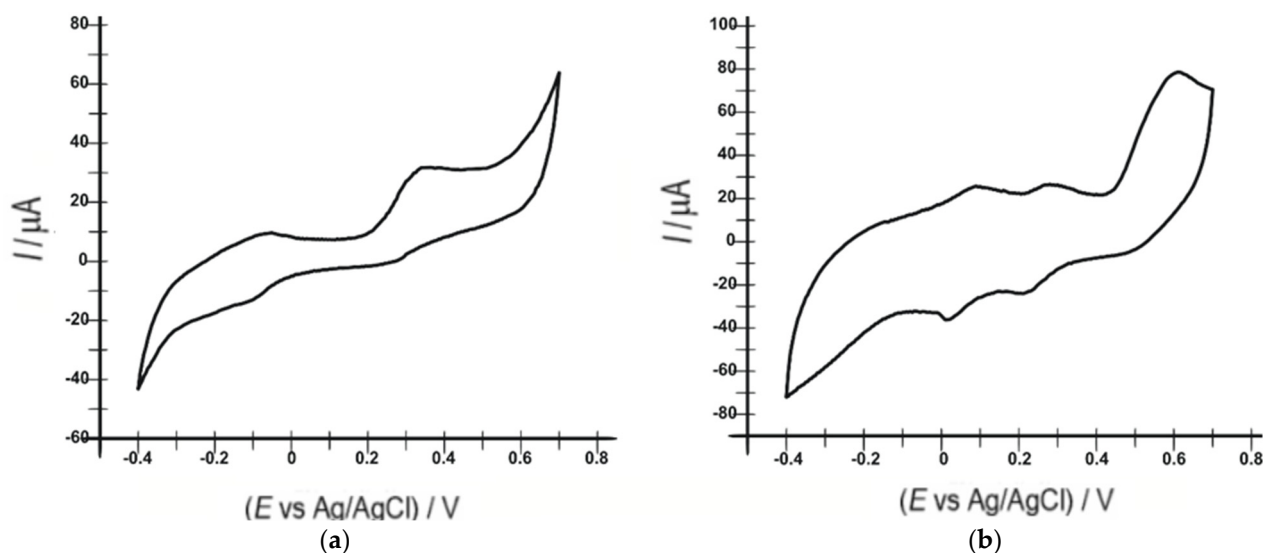


Figure 6. Cyclic voltammograms of OMC-SPE (a) and OMC-SPE/Lac (b) immersed in a 10^{-3} M serotonin solution and 0.1 M PBS at a $0.1 \text{ V}\cdot\text{s}^{-1}$ scan rate.

Figure 5 shows, in the case of the biosensor, two anodic peaks, with intensities of $25.76 \mu\text{A}$ at a potential of 0.091 V and $26.46 \mu\text{A}$ at a potential of 0.275 V , and two well-defined cathodic peaks, with intensities of $-35.99 \mu\text{A}$ at a potential of 0.018 V and $-23.47 \mu\text{A}$ at a potential of 0.217 V , corresponding to the oxidation and reduction of serotonin, favored by the presence of laccase on the surface of this modified electrode. In contrast, two anodic peaks, with intensities of $68.19 \mu\text{A}$ at a potential of -0.041 V and $112.05 \mu\text{A}$ at a potential of 0.394 V , and a single cathodic peak with an intensity of $-111.8 \mu\text{A}$ at a potential of -0.166 V were obtained with the unmodified sensor. In the case of the biosensor, another anodic peak with an intensity of $78.05 \mu\text{A}$ at a potential of $+0.6 \text{ V}$, characteristic of the determination of 5-HT due to the direct electron transfer to the T1 copper site of the laccase, was specified in the literature [69].

The biosensor was also used to record square-wave voltammograms in 10^{-3} M serotonin solution (Figure 7). SWV showed similar results to CV. Comparing the two voltammograms, the value of $-372.02 \mu\text{A}$ of the first cathodic peak in the SWV voltammogram at the potential of 0.018 V compared to the value of $-35.99 \mu\text{A}$ of the first cathodic peak in the CV voltammogram at the same potential is highlighted. The second cathodic peak in the SWV voltammogram occurred at a potential of 0.217 V with an intensity of $-335.71 \mu\text{A}$ as opposed to the second cathodic peak with an intensity of $-23.47 \mu\text{A}$ at the same potential

in the CV voltammogram. These data indicate an increased sensitivity of the biosensor to serotonin detection using the SWV technique.

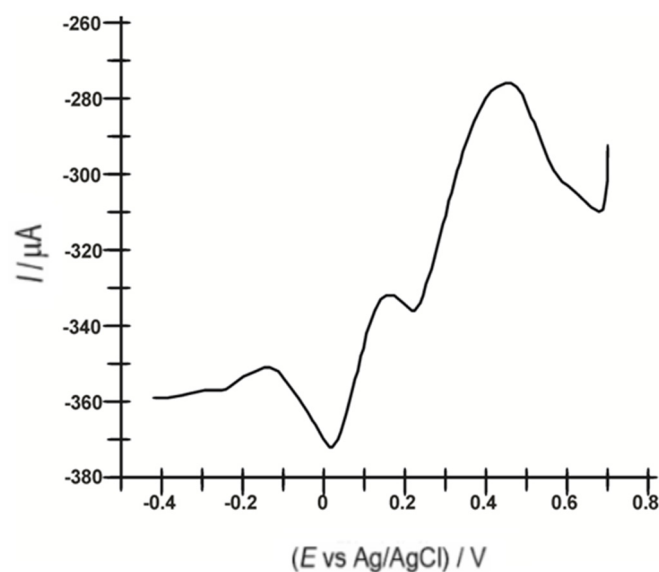


Figure 7. Square-wave voltammogram of OMC-SPE/Lac recorded in a 10^{-3} M serotonin solution and 0.1 M PBS.

The electrochemical oxidation of serotonin is presumed to occur at the phenolic group of the molecule to form quinone, and the presence of only one reduction peak at the unmodified electrode indicates the instability of this quinone, which is thought to undergo a chemical reaction to form an easily oxidized product. It is hypothesized that this readily oxidizable product is reduced hydroquinone [70].

Oxidoreductases, such as laccase, catalyze the transfer of electrons from one molecule, the reductant (also called the electron donor), to another, the oxidant (also called the electron acceptor). This redox process is notable for the appearance of specific electrochemical signals in both working electrodes used in this study, but it is more obvious when using the laccase-based biosensor.

Laccases catalyze the oxidation of ortho- and para-diphenols, aminophenols, polyphenols, polyamines, lignins, and aryl-diamines coupled with the reduction of molecular oxygen to water [47,71]. All laccase sublayers can be divided into two groups: (I) nonproton electron donors and (II) electron–proton donors [72]. The second group (II) includes phenols and aromatic amines, for which the potential has strong dependence on the *pH* of the solution. Hydroxylated indoleamines, such as serotonin, can be a substrate for electron transfer reactions that create radical-generating reactions [39].

Serotonin is a potent inducer of the redox process in the presence of redox-active compounds, such as copper, at the laccase site. Serotonin is a good substrate for oxidoreductases and produces reactive oxygen via oxygenase [39].

Direct electron transfer (DET), which takes place between the laccase and the electrode surface, favors electronic coupling between the enzyme and the electrode.

Laccase acts as an electrocatalyst, simplifying the transfer of electrons between the electrode and the substrate molecule, in this case serotonin, without the involvement of any mediator [73]. Biosensors based on the direct electron transfer process are therefore more selective and less prone to interference. They can operate in a potential range close to that of the enzyme [41].

Laccase includes four copper atoms: T1, T2, and two T3 atoms due to their spectroscopic properties. With higher potential values, the T1 copper center of the laccase can be reduced by phenol-derived compounds, one-electron redox mediators, and direct electron transfer from the electrodes [45,46].

In line with the above explanations, a laccase-catalyzed serotonin oxidation mechanism involving the transfer of two electrons and two protons in two steps, forming a quinone derivative, has been proposed (Figure 8).

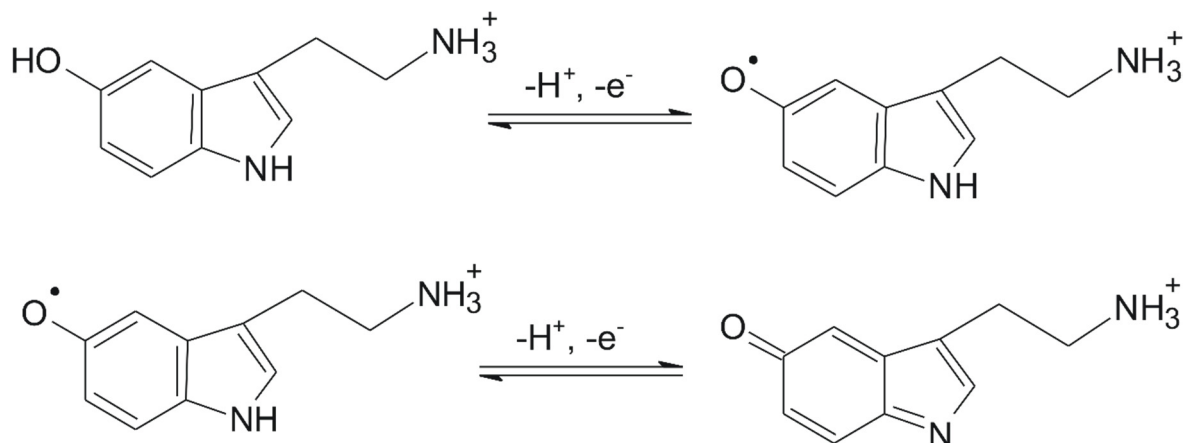


Figure 8. Electrochemical oxidation of serotonin [74].

Next, the influence of the scanning rate on the voltammetric response of the sensor and biosensor in a 10^{-3} M serotonin solution and 10^{-1} M PBS (*pH* 5.2) at a scanning rate between 0.1 and $1 \text{ V}\cdot\text{s}^{-1}$ was investigated. Figure 9 shows the obtained results.

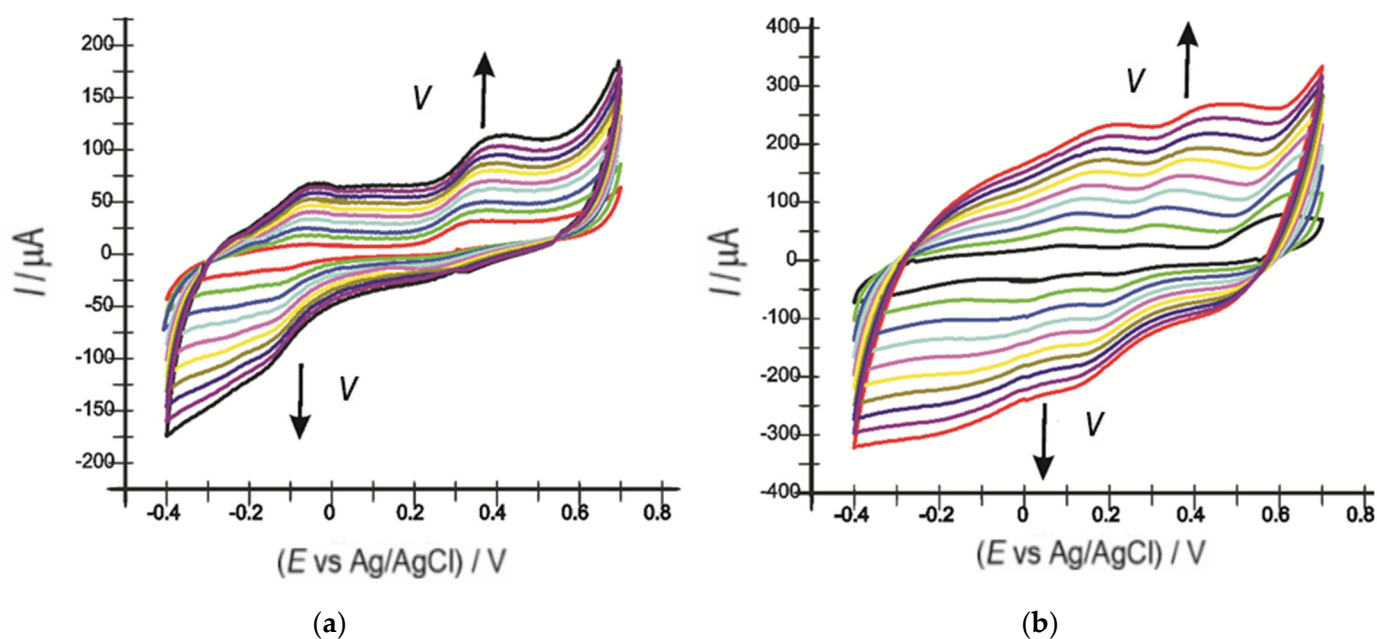


Figure 9. CVs recorded by OMC-SPE (a) and OMC-SPE/Lac (b) in a 10^{-3} M serotonin solution and 0.1 M PBS at different scan rates (0.1, 0.2, 0.3, 0.4, 0.5, 0.6, 0.7, 0.8, 0.9, and $1.0 \text{ V}\cdot\text{s}^{-1}$).

Laccase catalyzes the entire redox process of serotonin through the active surface of the electrode. Observing the cyclic voltammograms obtained with OMC-SPE and OMC-SPE/Lac, we found that a more obvious change occurs at the level of the cathodic peak.

In the case of the biosensor, a shift to the left of the cathodic peak potential was observed, a sign that the reduction process requires a lower activation energy [48,75].

Thus, the cathodic peak currents (I_c) of the two electrodes were plotted versus the scan rate. In the case of the biosensor, the cathodic peak occurring at a potential of $+0.012 \text{ V}$ was considered. A linear dependence between the cathodic peak intensities and the scan rate

was observed (Figure 10), demonstrating that the redox process of serotonin is controlled by electron transfer. Taking this into account, the Laviron equation was used to calculate the degree of surface coverage with the electroactive species (Γ).

$$I_c = \frac{n^2 F^2 \Gamma A v}{4RT}$$

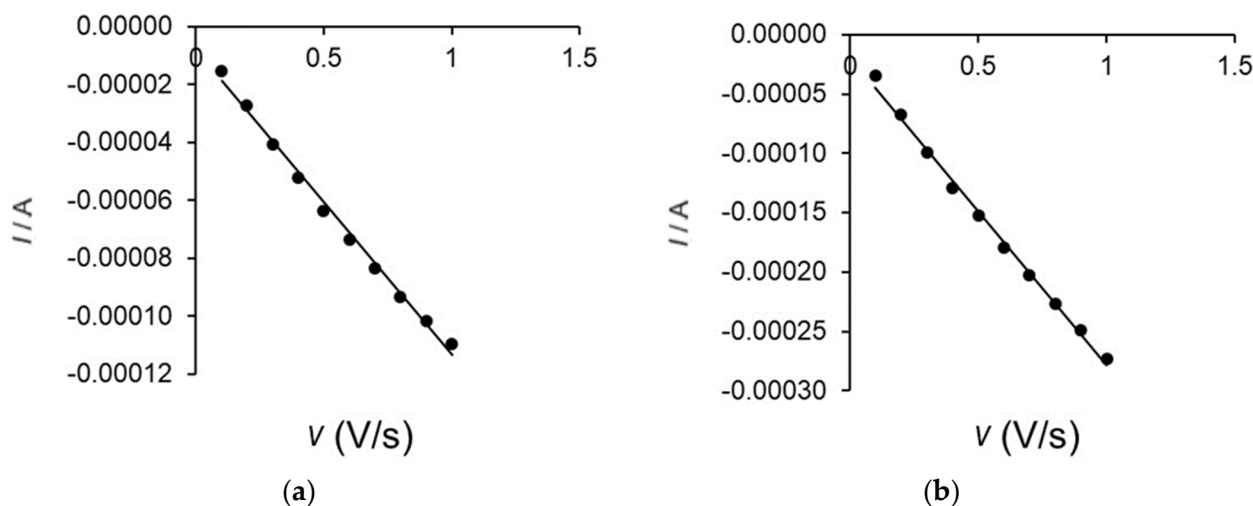


Figure 10. Linear dependence between cathodic current and scanning rate for OMC-SPE (a) and OMC-SPE/Lac (b).

The values shown in Table 3 indicate a higher Γ value for the OMC-SPE/Lac electrode compared to the unmodified OMC-SPE electrode, proving that the electron transfer-controlled redox process is faster in the case of the biosensor.

Table 3. Linear equation and degree of surface coverage with electroactive species.

Electrode	Linear Equation	R ²	Γ (mol·cm ⁻²)
OMC-SPE	$I = -1.053 \times 10^{-4}v - 8.111 \times 10^{-5}$	0.9944	3.09×10^{-10}
OMC-SPE/Lac	$I = -2.596 \times 10^{-4}v - 1.852 \times 10^{-5}$	0.9959	5.45×10^{-10}

3.5. Realization of the Calibration Curve

The influence of serotonin concentration on the electrochemical response of the biosensor was studied by square-wave voltammetry. Specifically, OMC-SPE/Lac was immersed in a PBS solution ($pH = 5.2$) to which different volumes of 10^{-3} M serotonin stock solution were successively added, and a square-wave voltammogram was recorded after each addition. The investigated concentration range was 0.1–10.48 μ M. Stable and reproducible SWV signals were obtained for all analyzed solutions. A linear increase of I_c with increasing concentrations in the range 0.1–1.2 μ M was observed, after which a maximum of the biosensor response was reached, at which the biosensor response did not change with increasing serotonin concentration. This is due to the depletion of the enzyme's active centers.

The calibration line was plotted over the range in which I_c increased linearly with concentration, i.e., 0.1–1.2 μ M. The plot of the dependence between I_c values and concentrations over the range of 0.1–1.2 μ M shows a linear dependence, and the correlation coefficient has a value of 0.9937, which is close to the ideal value of 1. From the slope of the calibration line in this concentration range, the limits of detection and quantification were calculated.

Figure 11 shows zoom of the cathodic peak zone of the square-wave voltammograms registered with OMC-SPE/Lac immersed in serotonin solutions in the range of 0.1–10.48 μ M (a), the dependence between cathodic peak currents and the concentration

of serotonin in the range of 0.1–10.48 μM (b), and the linear fits in the range of 0.1–1.2 μM (inset b) for OMC-SPE/Lac.

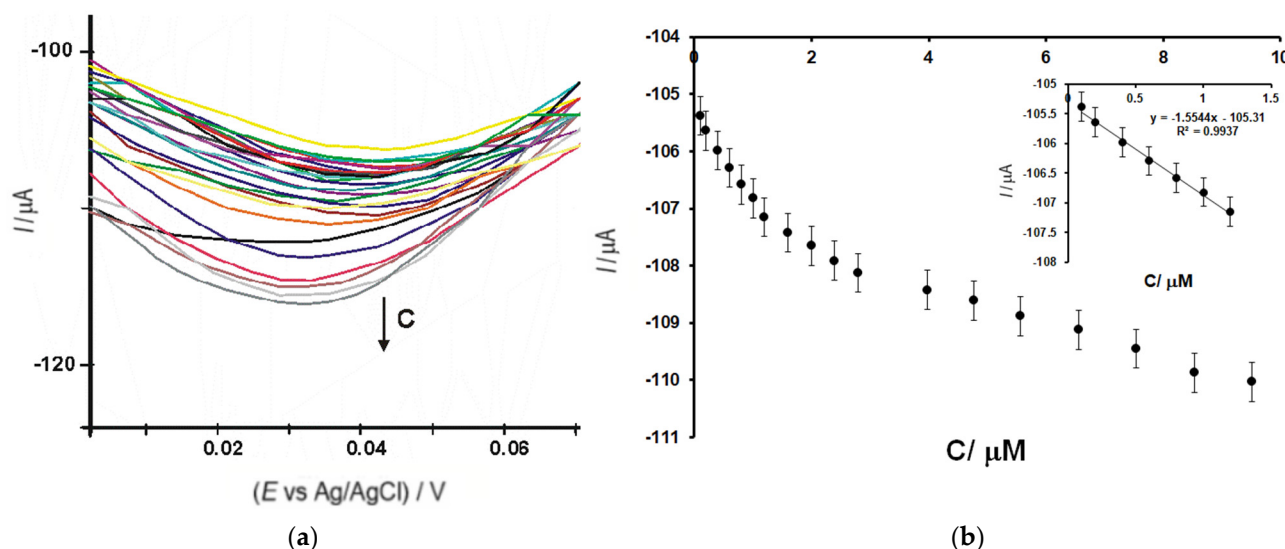


Figure 11. (a) Zoomed-in view of the cathodic peak zone of the square-wave voltammograms registered with OMC-SPE/Lac immersed in serotonin solutions with the concentrations in the 0.1–10.48 μM range; (b) I_c versus concentration in the range between 0.1 and 10.48 μM . Inset (b) shows the range of 0.1–1.2 μM (b) for OMC-SPE/Lac.

The detection limit was calculated to be $3\sigma/m$, and the quantification limit was calculated to be $10\sigma/m$, where m is the slope of the calibration equation and σ is the standard deviation ($n = 7$) [48,76,77] of the voltammetric signals corresponding to the lowest concentration.

The low LOD value of the biosensor shows a performance comparable to results obtained with other modified electrodes. These results are shown in Table 4:

Table 4. Main modified sensors used for serotonin determination with different voltammetric techniques.

Modified Electrode	Detection Technique	Linearity	LOD	Ref.
rGO-Ag ₂ Se ⁽¹⁾	DPV	0.1–15 μM	29.6 nM	[32]
GCE/CNFs ⁽²⁾	DPV	0.1–10 μM	250 nM	[78]
MWCNT ⁽³⁾ doped with Ni, Zn, and Fe	CV, SWV	0.006–62.8 μM	118 nM	[79]
Fe ₃ O ₄ NPs-MWCNT-poly(BOG) ⁽⁴⁾	DPV	0.5–100 μM	80 nM	[80]
MWCNT/CHT ⁽⁵⁾	CV, DPV	0.05–16 μM	50 nM	[81]
Pt-E/bisEDOTDTSi/Lac ⁽⁶⁾	CV	0.1–200 μM	48 nM	[39]
RGO/Co ₃ O ₄ nanocomposite ⁽⁷⁾	CV, DPV	0.1–51 μM	48.7 nM	[82]
OMC-SPE/Lac	SWV	0.1–1.2 μM	316 nM	This work

⁽¹⁾ reduced graphene oxide-silver selenide. ⁽²⁾ glassy carbon electrode (GCE)/carbon nanofibers (CNFs). ⁽³⁾ multiwall carbon nanotube (MWCNT). ⁽⁴⁾ Fe₃O₄ nanoparticles–multiwall carbon nanotubes–poly(bromocresol green). ⁽⁵⁾ multiwall carbon nanotube/chitosan. ⁽⁶⁾ platinum electrode/bis(3,4-ethylenedioxythiophene)-4-methyl-4-octyl-dithienosilole/laccase. ⁽⁷⁾ reduced graphene oxide/cobalt oxide nanocomposite.

Using the calibration data, the I_{max} (108.69 V) was determined and plotted as $\log[I/(I_{max} - I)]$ vs. $\log[\text{serotonin}]$. The slope of the obtained line represents the Hill coefficient (h). In the case of OMC-SPE/Lac, the Hill coefficient had a value of 0.90 ($R^2 = 0.952$) for the reduction process of the quinone derivative obtained from the enzymatic reaction at the biosensor surface. Given that the h -value is close to 1, the overall process at the biosensor surface exhibits Michaelis–Menten kinetics. The subunit value reflects a negative

cooperative effect between the occupied active zones on the OMC-SPE/Lac surface. Therefore, the Lineweaver–Burk equation was used to calculate the Michaelis–Menten constant:

$$\frac{1}{I} = \frac{1}{I_{max}} + \frac{K_M^{app}}{I_{max}[S]}$$

where I is the cathode current, I_{max} is the steady-state current, K_M^{app} is the apparent Michaelis–Menten constant, and $[S]$ is the substrate concentration. From the ordinate of the origin, the value of I_{max} was calculated, and from the slope of the line, the value of K_M^{app} was calculated. The characteristic parameters of OMC-SPE/Lac for serotonin are given in Table 5.

Table 5. OMC-SPE/Lac characteristic parameters for serotonin.

Studied Compound	OMC-SPE/Lac		
	h (Hill Coefficient)	$I_{max}/\mu\text{A}$	$K_M^{app}/\mu\text{M}$
Serotonin	0.90	108.6957	0.01087

The low value of the Michaelis–Menten constant indicates that the affinity between laccase and serotonin is strong for the biosensor.

3.6. Stability, Repeatability and Interference Studies

The stability of the OMC-SPE/Lac biosensor was investigated by performing 50 cyclic voltammetry measurements using a 10^{-6} M serotonin solution. The results indicated that the biosensor maintained its stability throughout the determinations, with no significant differences between the cathodic currents considered.

Solutions of different concentrations of several amino acids found with serotonin in commercial products, e.g., tyrosine, tryptophan, and phenylalanine, were used in the interference studies. The results in Table 6 indicate that the corresponding serotonin peaks do not change significantly due to the added interferents.

Table 6. Interference of chemically related substances in the detection of serotonin concentration (10^{-6} M).

Interfering Compound	Concentration/M	Recovery/%	RSD/%	Tolerance Limit/M
				(Concentration of Interferent That Determined an RSD of 5%)
Tyrosine	10^{-5}	99.8	2.7	1.85×10^{-5}
Tryptophan	10^{-5}	97.4	3.2	1.56×10^{-5}
Phenylalanine	10^{-5}	100.2	2.9	1.72×10^{-5}

3.7. Determination of Serotonin from Real Samples

Considering the superior properties of OMC-SPE/Lac, this biosensor has been used in the following analyses for the quantitative determination of serotonin in dietary supplements (Now Foods, Bio Raw Foods, and Haya Labs). The contents of the capsules were dissolved and homogenized to obtain solutions. These solutions were analyzed with the OMC-SPE/Lac biosensor by square-wave voltammetry. The results from the voltammetric method were compared with those from the FTIR method to validate the electrochemical method for the serotonin analysis of real samples.

The square-wave voltammograms recorded with OMC-SPE/Lac shown in Figure 11 indicate the reduction peak of serotonin in the solution to be analyzed, which occurred at the same potential value (0.018 V) as in the standard samples. The second peak observed in SWV was due to the L-Dopa present in the natural product. The manufacturer indicates the presence of this compound in the analyzed samples, and it was determined in a previous study [83].

Figure 12 shows the square-wave voltammograms of the OMC-SPE/Lac introduced into solutions of different concentrations of Now Foods, Bio Raw Foods, and Haya Labs products.

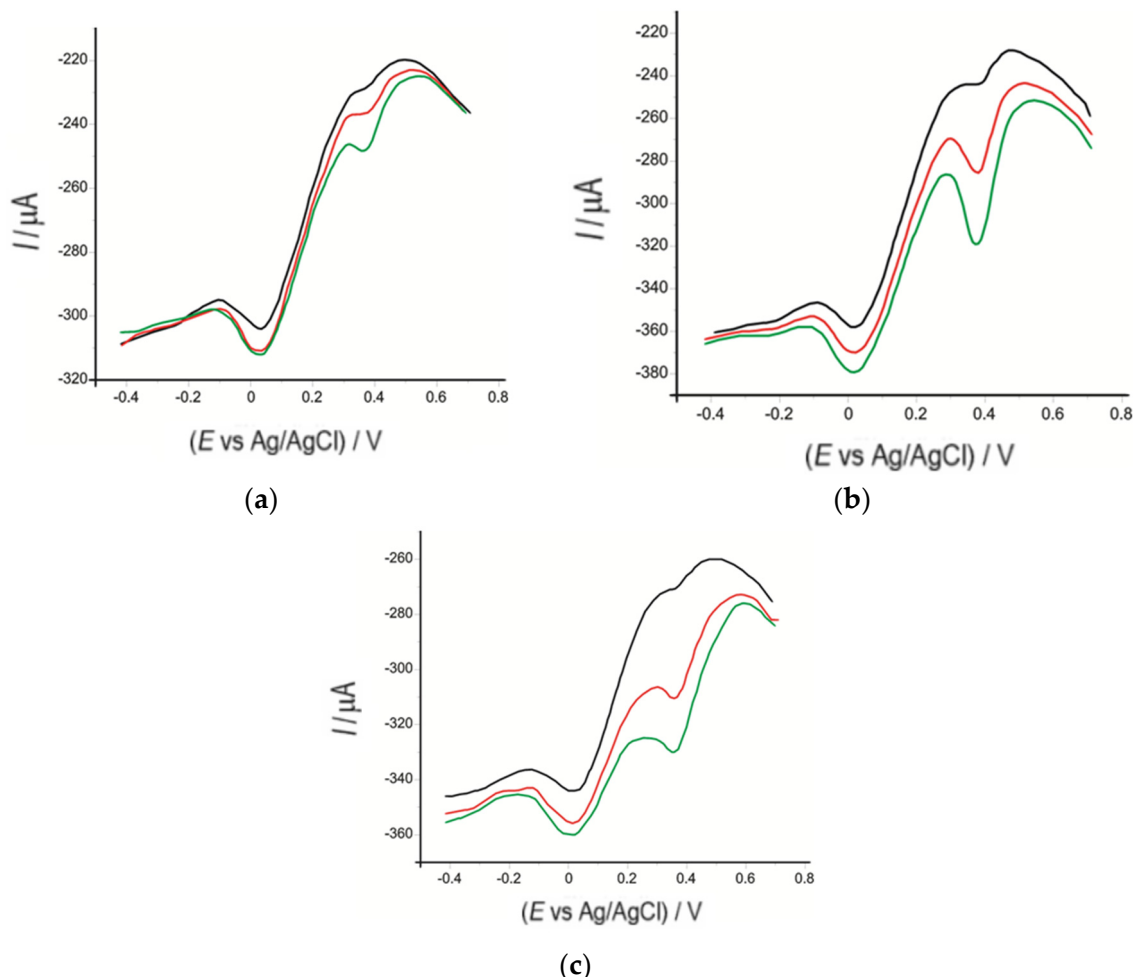


Figure 12. Square-wave voltammograms of OMC-SPCE/Lac immersed in solutions of (a) Bio Raw Foods, (b) Haya Labs, and (c) Now Foods products containing different amounts: 0.015 g (black line), 0.035 g (red line), 0.055 g (green line), with each amount dissolved in 50 mL of 10^{-1} M PBS (pH 5.2).

The most intense cathodic peak current was used to quantify serotonin from the dietary supplements mentioned above. Table 7 shows the obtained results.

Table 7. Serotonin concentrations obtained by FTIR and voltammetric methods.

Food Supplement	c% Serotonin FTIR Method	c% Serotonin Voltammetric Method
Now Foods	1.42	1.50
Bio Raw Foods	1.25	1.52
Haya Labs	1.48	1.44

The feasibility and accuracy of the voltammetric method was verified with the FTIR spectrometric method.

FTIR is an analytical test application generally used to identify the chemical properties of substances/materials. Similar to other substances, serotonin, through its functional groups, generates a unique spectral imprint and is easy to identify. Studying the obtained spectrum, the wavelength of 3285 cm^{-1} was selected as being representative of the presence

of serotonin. Making a calibration curve with the help of the absorbents measured for different concentrations of serotonin, the quantification of the biogenic amine from the selected real samples was achieved. The quantitative determination of some analytes has often been reported in the literature [48,84,85]. Figure 13 shows the FTIR spectra of analyzed samples from Now Foods, Bio Raw Foods, and Haya Labs food supplements.

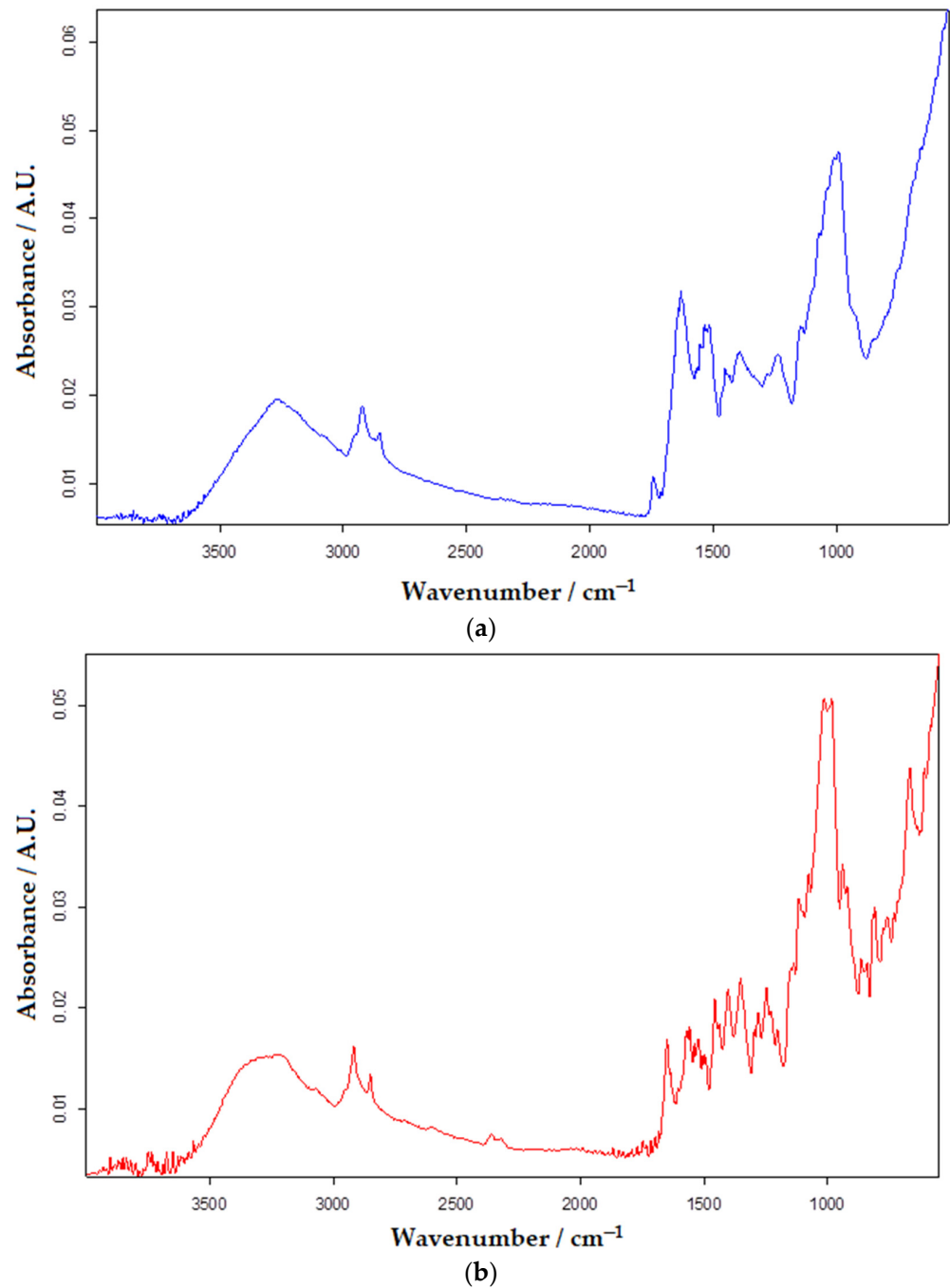


Figure 13. Cont.

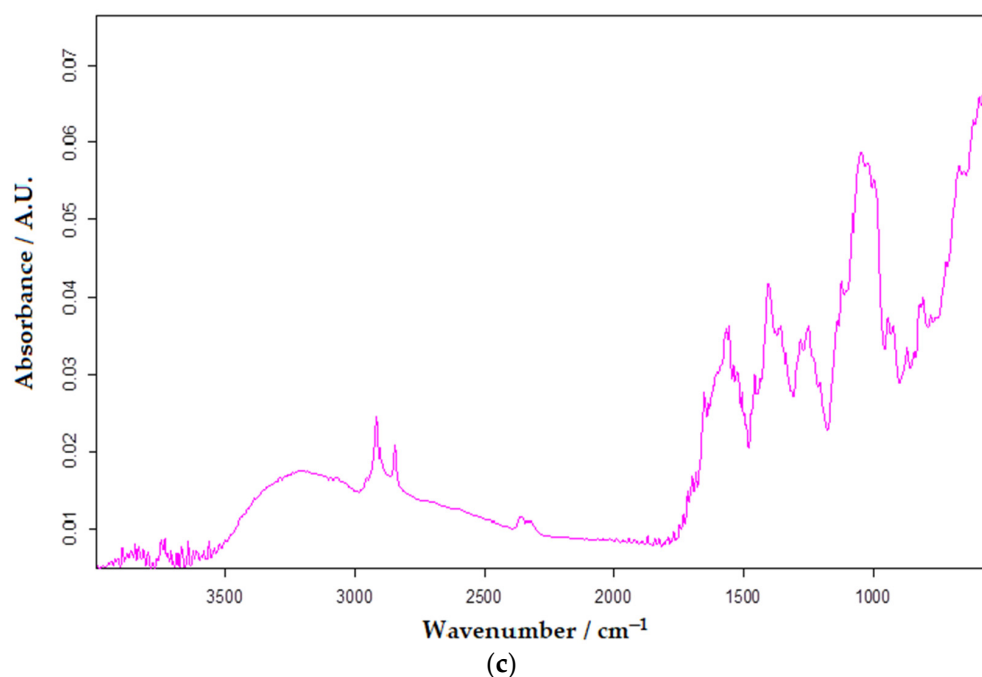


Figure 13. FTIR spectra of analyzed samples from Now Foods (a), Bio Raw Foods (b), and Haya Labs (c) dietary supplements.

The results obtained by the FTIR method are close in value to those from square-wave voltammetry using the OMC-SPE/Lac biosensor.

4. Conclusions

In this work, the electrochemical performance of a novel screen-printed carbon-based electrode modified with laccase (OMC-SPE/Lac) was studied and compared with that of an unmodified carbon-based screen-printed electrode (OMC-SPE). Electrochemical process kinetics studies confirmed the superiority of the OMC-SPE/Lac biosensor over the unmodified OMC-SPE sensor, and consequently it was used for the quantitative determination of serotonin in three dietary supplements. The FTIR spectrometric method was used in the validation step, and it confirmed the accuracy of the voltammetric method, which obtained similar results.

Author Contributions: Conceptualization, C.A.; methodology, C.A.; validation, C.A. and D.D.; formal analysis, D.D.; investigation, C.A. and D.D.; data curation, C.A. and D.D.; writing—original draft preparation, D.D.; writing—review and editing, C.A.; supervision, C.A. All authors have read and agreed to the published version of the manuscript.

Funding: This work was supported by a grant from the Romanian Ministry of Education and Research, CNCS—UEFISCDI, project number PN-III-P4-ID-PCE-2020-0923, within PNCDI III.

Institutional Review Board Statement: Not applicable.

Informed Consent Statement: Not applicable.

Data Availability Statement: Not applicable.

Conflicts of Interest: The authors declare no conflict of interest.

References

1. Shajib, M.S.; Baranov, A.; Khan, W.I. Diverse Effects of Gut-Derived Serotonin in Intestinal Inflammation. *ACS Chem. Neurosci.* **2017**, *8*, 920–931. [[CrossRef](#)] [[PubMed](#)]
2. Ramage, A.G. The Role of Central 5-Hydroxytryptamine (5-HT, Serotonin) Receptors in the Control of Micturition: 5-HT Receptors and Micturition. *Br. J. Pharmacol.* **2006**, *147*, S120–S131. [[CrossRef](#)] [[PubMed](#)]

3. Lindström, M.; Tohmola, N.; Renkonen, R.; Hämäläinen, E.; Schalin-Jäntti, C.; Itkonen, O. Comparison of Serum Serotonin and Serum 5-HIAA LC-MS/MS Assays in the Diagnosis of Serotonin Producing Neuroendocrine Neoplasms: A Pilot Study. *Clin. Chim. Acta* **2018**, *482*, 78–83. [[CrossRef](#)] [[PubMed](#)]
4. Brand, T.; Anderson, G.M. The Measurement of Platelet-Poor Plasma Serotonin: A Systematic Review of Prior Reports and Recommendations for Improved Analysis. *Clin. Chem.* **2011**, *57*, 1376–1386. [[CrossRef](#)]
5. Huang, H.; Chen, Z.; Yan, X. Simultaneous Determination of Serotonin and Creatinine in Urine by Combining Two Ultrasound-Assisted Emulsification Microextractions with on-Column Stacking in Capillary Electrophoresis: Electrodriven Separations. *J. Sep. Sci.* **2012**, *35*, 436–444. [[CrossRef](#)]
6. Rognum, I.J.; Tran, H.; Haas, E.A.; Hyland, K.; Paterson, D.S.; Haynes, R.L.; Broadbelt, K.G.; Harty, B.J.; Mena, O.; Krous, H.F.; et al. Serotonin Metabolites in the Cerebrospinal Fluid in Sudden Infant Death Syndrome. *J. Neuropathol. Exp. Neurol.* **2014**, *73*, 115–122. [[CrossRef](#)]
7. Jones, B.J.; Blackburn, T.P. The Medical Benefit of 5-HT Research. *Pharmacol. Biochem. Behav.* **2002**, *71*, 555–568. [[CrossRef](#)]
8. Lin, S.H.; Lee, L.T.; Yang, Y.K. Serotonin and Mental Disorders: A Concise Review on Molecular Neuroimaging Evidence. *Clin. Psychopharmacol. Neurosci.* **2014**, *12*, 196–202. [[CrossRef](#)]
9. Squires, L.N.; Talbot, K.N.; Rubakhin, S.S.; Sweedler, J.V. Serotonin Catabolism in the Central and Enteric Nervous Systems of Rats upon Induction of Serotonin Syndrome. *J. Neurochem.* **2007**, *103*, 174–180. [[CrossRef](#)]
10. Feldman, J.M.; Lee, E.M. Serotonin Content of Foods: Effect on Urinary Excretion of 5-Hydroxyindoleacetic Acid. *Am. J. Clin. Nutr.* **1985**, *42*, 639–643. [[CrossRef](#)]
11. Ávila, M.; Crevillén, A.G.; González, M.C.; Escarpa, A.; Hortigüela, L.V.; de Lorenzo Carretero, C.; Pérez Martín, R.A. Electroanalytical Approach to Evaluate Antioxidant Capacity in Honeys: Proposal of an Antioxidant Index. *Electroanalysis* **2006**, *18*, 1821–1826. [[CrossRef](#)]
12. Ghosal, S.; Singh, S.; Bhattacharya, S. Alkaloids of *Mucuna pruriens* chemistry and pharmacology. *Planta Med.* **1971**, *19*, 279–284. [[CrossRef](#)]
13. Bottiglieri, T.; Lim, C.K.; Peters, T.J. Isocratic Analysis of 3-Methoxy-4-Hydroxyphenyl Glycol, 5-Hydroxyindole-3-Acetic Acid and 4-Hydroxy-3-Methoxyphenylacetic Acid in Cerebrospinal Fluid by High-Performance Liquid Chromatography with Amperometric Detection. *J. Chromatogr. B Biomed. Sci. Appl.* **1984**, *311*, 354–360. [[CrossRef](#)]
14. Brashear, J.; Zeitvogel, C.; Jackson, J.; Flentge, C.; Janulis, L.; Cantrell, L.; Schmidt, B.; Adamczyk, M.; Betebenner, D.; Vaughan, K. Fluorescence Polarization Immunoassay of Urinary 5-Hydroxy-3-Indoleacetic Acid. *Clin. Chem.* **1989**, *35*, 355–359. [[CrossRef](#)]
15. He, Q.; Li, M.; Wang, X.; Xia, Z.; Du, Y.; Li, Y.; Wei, L.; Shang, J. A Simple, Efficient and Rapid HPLC–UV Method for the Detection of 5-HT in RIN-14B Cell Extract and Cell Culture Medium. *BMC Chem.* **2019**, *13*, 76. [[CrossRef](#)]
16. Ma, L.; Zhao, T.; Zhang, P.; Liu, M.; Shi, H.; Kang, W. Determination of Monoamine Neurotransmitters and Metabolites by High-Performance Liquid Chromatography Based on Ag(III) Complex Chemiluminescence Detection. *Anal. Biochem.* **2020**, *593*, 113594. [[CrossRef](#)] [[PubMed](#)]
17. Roychoudhury, A.; Francis, K.A.; Patel, J.; Jha, S.K.; Basu, S. A Decoupler-Free Simple Paper Microchip Capillary Electrophoresis Device for Simultaneous Detection of Dopamine, Epinephrine and Serotonin. *RSC Adv.* **2020**, *10*, 25487–25495. [[CrossRef](#)]
18. Piešťanský, J.; Maráková, K.; Mikuš, P. Two-Dimensional Capillary Electrophoresis with On-Line Sample Preparation and Cyclodextrin Separation Environment for Direct Determination of Serotonin in Human Urine. *Molecules* **2017**, *22*, 1668. [[CrossRef](#)]
19. Zhang, L.; Zhao, Y.; Huang, J.; Zhao, S. Simultaneous Quantification of 5-Hydroxyindoleacetic Acid and 5-Hydroxytryptamine by Capillary Electrophoresis with Quantum Dot and Horseradish Peroxidase Enhanced Chemiluminescence Detection. *J. Chromatogr. B* **2014**, *967*, 190–194. [[CrossRef](#)]
20. Zinellu, A.; Sotgia, S.; Deiana, L.; Carru, C. Reverse Injection Capillary Electrophoresis UV Detection for Serotonin Quantification in Human Whole Blood. *J. Chromatogr. B* **2012**, *895–896*, 182–185. [[CrossRef](#)]
21. Darwish, I.A.; Refaat, I.H. Spectrophotometric Analysis of Selective Serotonin Reuptake Inhibitors Based on Formation of Charge-Transfer Complexes with Tetracyanoquinodimethane and Chloranilic Acid. *J. AOAC Int.* **2006**, *89*, 326–333. [[CrossRef](#)] [[PubMed](#)]
22. Zhao, Y.Y.; Li, H.; Ge, Q.M.; Cong, H.; Liu, M.; Tao, Z.; Zhao, J.L. A Chemo-Sensor Constructed by Nanohybrid of Multifarene[3,3] and RGO for Serotonin Hydrochloride with Dual Response in Both Fluorescence and Voltammetry. *Microchem. J.* **2020**, *158*, 105145. [[CrossRef](#)]
23. Sha, Q.; Sun, B.; Yi, C.; Guan, R.; Fei, J.; Hu, Z.; Liu, B.; Liu, X. A Fluorescence Turn-on Biosensor Based on Transferrin Encapsulated Gold Nanoclusters for 5-Hydroxytryptamine Detection. *Sens. Actuators B Chem.* **2019**, *294*, 177–184. [[CrossRef](#)]
24. Wang, Z.; Zhang, Y.; Zhang, B.; Lu, X. Mn²⁺ Doped ZnS QDs Modified Fluorescence Sensor Based on Molecularly Imprinted Polymer/Sol-Gel Chemistry for Detection of Serotonin. *Talanta* **2018**, *190*, 1–8. [[CrossRef](#)] [[PubMed](#)]
25. Wu, D.; Xie, H.; Lu, H.; Li, W.; Zhang, Q. Sensitive Determination of Norepinephrine, Epinephrine, Dopamine and 5-Hydroxytryptamine by Coupling HPLC with [Ag(HIO₆)₂]⁵⁻-Luminol Chemiluminescence Detection: Sensitive Detection of Monoamine Neurotransmitters by HPLC-CL Method. *Biomed. Chromatogr.* **2016**, *30*, 1458–1466. [[CrossRef](#)]
26. Labib, M.; Sargent, E.H.; Kelley, S.O. Electrochemical Methods for the Analysis of Clinically Relevant Biomolecules. *Chem. Rev.* **2016**, *116*, 9001–9090. [[CrossRef](#)]
27. Vilas-Boas, Â.; Valderrama, P.; Fontes, N.; Geraldo, D.; Bento, F. Evaluation of Total Polyphenol Content of Wines by Means of Voltammetric Techniques: Cyclic Voltammetry vs Differential Pulse Voltammetry. *Food Chem.* **2019**, *276*, 719–725. [[CrossRef](#)]

28. Mirceski, V.; Skrzypek, S.; Stojanov, L. Square-Wave Voltammetry. *ChemTexts* **2018**, *4*, 101–110. [CrossRef]
29. Bounegru, A.V.; Apetrei, C. Sensitive Detection of Hydroxytyrosol in Extra Virgin Olive Oils with a Novel Biosensor Based on Single-Walled Carbon Nanotubes and Tyrosinase. *IJMS* **2022**, *23*, 9132. [CrossRef]
30. Wu, B.; Yeasmin, S.; Liu, Y.; Cheng, L.J. Sensitive and Selective Electrochemical Sensor for Serotonin Detection Based on Ferrocene-Gold Nanoparticles Decorated Multiwall Carbon Nanotubes. *Sens. Actuators B Chem.* **2022**, *354*, 131216. [CrossRef]
31. Moslah, M.; Fredj, Z.; Dridi, C. Development of a New Highly Sensitive Serotonin Sensor Based on Green Synthesized Silver Nanoparticle Decorated Reduced Graphene Oxide. *Anal. Methods* **2021**, *13*, 5187–5194. [CrossRef] [PubMed]
32. Panneer Selvam, S.; Yun, K. A Self-Assembled Silver Chalcogenide Electrochemical Sensor Based on RGO-Ag₂Se for Highly Selective Detection of Serotonin. *Sens. Actuators B Chem.* **2020**, *302*, 127161. [CrossRef]
33. Uwaya, G.E.; Fayemi, O.E. Electrochemical Detection of Serotonin in Banana at Green Mediated PPy/Fe₃O₄NPs Nanocomposites Modified Electrodes. *Sens. Bio-Sens. Res.* **2020**, *28*, 100338. [CrossRef]
34. Selvarajan, S.; Suganthi, A.; Rajarajan, M. A Novel Highly Selective and Sensitive Detection of Serotonin Based on Ag/Polypyrrole/Cu₂O Nanocomposite Modified Glassy Carbon Electrode. *Ultrason. Sonochem.* **2018**, *44*, 319–330. [CrossRef]
35. Lavanya, N.; Sekar, C. SnO₂-SnS₂ Nanocomposite as Electrocatalyst for Simultaneous Determination of Depression Biomarkers Serotonin and Tryptophan. *J. Electroanal. Chem.* **2019**, *840*, 1–9. [CrossRef]
36. Arvand, M.; Samie, H.A. Electrospun CeO₂-Au Nanofibers/Graphene Oxide 3D Nanonetwork Structure for the Electrocatalytic Detection of Amlodipine. *Ionics* **2018**, *24*, 1813–1826. [CrossRef]
37. Ramos, M.M.V.; Carvalho, J.H.S.; de Oliveira, P.R.; Janegitz, B.C. Determination of Serotonin by Using a Thin Film Containing Graphite, Nanodiamonds and Gold Nanoparticles Anchored in Casein. *Measurement* **2020**, *149*, 106979. [CrossRef]
38. Castilho, T.J.; Sotomayor, M.D.P.T.; Kubota, L.T. Amperometric Biosensor Based on Horseradish Peroxidase for Biogenic Amine Determinations in Biological Samples. *J. Pharm. Biomed. Anal.* **2005**, *37*, 785–791. [CrossRef]
39. Baluta, S.; Zając, D.; Szyszka, A.; Malecha, K.; Cabaj, J. Enzymatic Platforms for Sensitive Neurotransmitter Detection. *Sensors* **2020**, *20*, 423. [CrossRef]
40. Chávez, J.; Hagen, J.; Kelley-Loughnane, N. Fast and Selective Plasmonic Serotonin Detection with Aptamer-Gold Nanoparticle Conjugates. *Sensors* **2017**, *17*, 681. [CrossRef]
41. Freire, R.S.; Pessoa, C.A.; Mello, L.D.; Kubota, L.T. Direct Electron Transfer: An Approach for Electrochemical Biosensors with Higher Selectivity and Sensitivity. *J. Braz. Chem. Soc.* **2003**, *14*, 230–243. [CrossRef]
42. Xu, F.; Shin, W.; Brown, S.H.; Wahleithner, J.A.; Sundaram, U.M.; Solomon, E.I. A Study of a Series of Recombinant Fungal Laccases and Bilirubin Oxidase That Exhibit Significant Differences in Redox Potential, Substrate Specificity, and Stability. *Biochim. Biophys. Acta (BBA)-Protein Struct. Mol. Enzymol.* **1996**, *1292*, 303–311. [CrossRef]
43. Varfolomeev, S.D.; Kurochkin, I.N.; Yaropolov, A.I. Direct Electron Transfer Effect Biosensors. *Biosens. Bioelectron.* **1996**, *11*, 863–871. [CrossRef]
44. Lee, C.W.; Gray, H.B.; Anson, F.C.; Malmström, B.G. Catalysis of the Reduction of Dioxygen at Graphite Electrodes Coated with Fungal Laccase A. *J. Electroanal. Chem. Interfac. Electrochem.* **1984**, *172*, 289–300. [CrossRef]
45. Gallaway, J.W.; Calabrese Barton, S.A. Kinetics of Redox Polymer-Mediated Enzyme Electrodes. *J. Am. Chem. Soc.* **2008**, *130*, 8527–8536. [CrossRef]
46. Mano, N.; Soukharev, V.; Heller, A. A Laccase-Wiring Redox Hydrogel for Efficient Catalysis of O₂ Electroreduction. *J. Phys. Chem. B* **2006**, *110*, 11180–11187. [CrossRef]
47. Solomon, E.I.; Sundaram, U.M.; Machonkin, T.E. Multicopper Oxidases and Oxygenases. *Chem. Rev.* **1996**, *96*, 2563–2606. [CrossRef] [PubMed]
48. Bounegru, A.V.; Apetrei, C. Development of a Novel Electrochemical Biosensor Based on Carbon Nanofibers–Cobalt Phthalocyanine–Laccase for the Detection of p-Coumaric Acid in Phytoproducts. *Int. J. Mol. Sci.* **2021**, *22*, 9302. [CrossRef] [PubMed]
49. Sun, J.; Yang, L.; Jiang, M.; Shi, Y.; Xu, B.; Ma, H. Stability and Activity of Immobilized Trypsin on Carboxymethyl Chitosan-Functionalized Magnetic Nanoparticles Cross-Linked with Carbodiimide and Glutaraldehyde. *J. Chromatogr. B* **2017**, *1054*, 57–63. [CrossRef]
50. Mucuna Pruriens Pulbere Ecologica/Bio 125 g Obio-Natural-Vegis.ro. Available online: <https://vegis.ro/suplimente-pulbere/obio/11253-mucuna-pruriens-pulbere-ecologica-bio-125g/> (accessed on 11 July 2022).
51. Borah, M.M.; Devi, T.G. Vibrational Study and Natural Bond Orbital Analysis of Serotonin in Monomer and Dimer States by Density Functional Theory. *J. Mol. Struct.* **2018**, *1161*, 464–476. [CrossRef]
52. Pan, M.; Shan, C.; Zhang, X.; Zhang, Y.; Zhu, C.; Gao, G.; Pan, B. Environmentally Friendly In Situ Regeneration of Graphene Aerogel as a Model Conductive Adsorbent. *Environ. Sci. Technol.* **2018**, *52*, 739–746. [CrossRef] [PubMed]
53. Li, X.; Zhang, W.; Xie, D.; Wang, X.; Ye, W.; Liang, W. Electrochemical Treatment of Humic Acid Using Particle Electrodes Ensembled by Ordered Mesoporous Carbon. *Environ. Sci. Pollut. Res.* **2018**, *25*, 20071–20083. [CrossRef] [PubMed]
54. Mosallanejad, S.; Długogorski, B.Z.; Kennedy, E.M.; Stockenhuber, M. Adsorption of 2-Chlorophenol on the Surface of Silica- and Alumina-Supported Iron Oxide: An FTIR and XPS Study. *ChemCatChem* **2017**, *9*, 481–491. [CrossRef]
55. Kong, J.; Yu, S. Fourier Transform Infrared Spectroscopic Analysis of Protein Secondary Structures. *Acta Biochim. Biophys. Sin.* **2007**, *39*, 549–559. [CrossRef]

56. Susi, H.; Byler, D.M. [13] Resolution-Enhanced Fourier Transform Infrared Spectroscopy of Enzymes. In *Methods in Enzymology*; Elsevier: Amsterdam, The Netherlands, 1986; Volume 130, pp. 290–311. ISBN 978-0-12-182030-5.
57. Surewicz, W.K.; Mantsch, H.H. New Insight into Protein Secondary Structure from Resolution-Enhanced Infrared Spectra. *Biochim. Biophys. Acta (BBA)-Protein Struct. Mol. Enzymol.* **1988**, *952*, 115–130. [[CrossRef](#)]
58. Krimm, S.; Bandekar, J. Vibrational Spectroscopy and Conformation of Peptides, Polypeptides, and Proteins. In *Advances in Protein Chemistry*; Elsevier: Amsterdam, The Netherlands, 1986; Volume 38, pp. 181–364. ISBN 978-0-12-034238-9.
59. Ramasubramaniam, S.; Govindarajan, C.; Nasreen, K.; Sudha, P.N. Removal of Cadmium (II) Ions from Aqueous Solution Using Chitosan/Starch Polymer Blend. *Compos. Interfaces* **2014**, *21*, 95–109. [[CrossRef](#)]
60. Thiagarajan, P.; Selvam, K.; Sudhakar, C.; Selvankumar, T. Enhancement of Adsorption of Magenta Dye by Immobilized Laccase on Functionalized Biosynthesized Activated Carbon Nanotubes. *Water Air Soil Pollut.* **2020**, *231*, 364. [[CrossRef](#)]
61. Huang, H.; Chen, Y.; Chen, Z.; Chen, J.; Hu, Y.; Zhu, J.J. Electrochemical Sensor Based on Ce-MOF/Carbon Nanotube Composite for the Simultaneous Discrimination of Hydroquinone and Catechol. *J. Hazard. Mater.* **2021**, *416*, 125895. [[CrossRef](#)]
62. Wang, F.; Wu, Y.; Lu, K.; Ye, B. A Simple but Highly Sensitive and Selective Calixarene-Based Voltammetric Sensor for Serotonin. *Electrochim. Acta* **2013**, *87*, 756–762. [[CrossRef](#)]
63. Han, S.; Zhang, T.; Li, T.; Kong, L.; Lv, Y.; He, L. A Sensitive HPLC-ECD Method for Detecting Serotonin Released by RBL-2H3 Cells Stimulated by Potential Allergens. *Anal. Methods* **2015**, *7*, 8918–8924. [[CrossRef](#)]
64. Gunache (Roșca), R.O.; Bounegru, A.V.; Apetrei, C. Determination of Atorvastatin with Voltammetric Sensors Based on Nanomaterials. *Inventions* **2021**, *6*, 57. [[CrossRef](#)]
65. Munteanu, I.G.; Apetrei, C. Electrochemical Determination of Chlorogenic Acid in Nutraceuticals Using Voltammetric Sensors Based on Screen-Printed Carbon Electrode Modified with Graphene and Gold Nanoparticles. *Int. J. Mol. Sci.* **2021**, *22*, 8897. [[CrossRef](#)] [[PubMed](#)]
66. Burestedt, E.; Narvaez, A.; Ruzgas, T.; Gorton, L.; Emnéus, J.; Domínguez, E.; Marko-Varga, G. Rate-Limiting Steps of Tyrosinase-Modified Electrodes for the Detection of Catechol. *Anal. Chem.* **1996**, *68*, 1605–1611. [[CrossRef](#)] [[PubMed](#)]
67. Łukaszewski, M.; Soszko, M.; Czerwiński, A. Electrochemical Methods of Real Surface Area Determination of Noble Metal Electrodes—An Overview. *Int. J. Electrochem. Sci.* **2016**, *11*, 4442–4469. [[CrossRef](#)]
68. Anithaa, A.C.; Asokan, K.; Sekar, C. Highly Sensitive and Selective Serotonin Sensor Based on Gamma Ray Irradiated Tungsten Trioxide Nanoparticles. *Sens. Actuators B Chem.* **2017**, *238*, 667–675. [[CrossRef](#)]
69. Adam, C.; Scodeller, P.; Grattieri, M.; Villalba, M.; Calvo, E.J. Revisiting Direct Electron Transfer in Nanostructured Carbon Laccase Oxygen Cathodes. *Bioelectrochemistry* **2016**, *109*, 101–107. [[CrossRef](#)]
70. Sarada, B.V.; Rao, T.N.; Tryk, D.A.; Fujishima, A. Electrochemical Oxidation of Histamine and Serotonin at Highly Boron-Doped Diamond Electrodes. *Anal. Chem.* **2000**, *72*, 1632–1638. [[CrossRef](#)]
71. Yaropolov, A.I.; Skorobogat'ko, O.V.; Vartanov, S.S.; Varfolomeyev, S.D. Laccase: Properties, Catalytic Mechanism, and Applicability. *Appl. Biochem. Biotechnol.* **1994**, *49*, 257–280. [[CrossRef](#)]
72. Xu, F.; Kulys, J.J.; Duke, K.; Li, K.; Krikstopaitis, K.; Deussen, H.J.W.; Abbate, E.; Galinyte, V.; Schneider, P. Redox Chemistry in Laccase-Catalyzed Oxidation of N-Hydroxy Compounds. *Appl. Environ. Microbiol.* **2000**, *66*, 2052–2056. [[CrossRef](#)]
73. Ghindilis, A.L.; Atanasov, P.; Wilkins, E. Enzyme-Catalyzed Direct Electron Transfer: Fundamentals and Analytical Applications. *Electroanalysis* **1997**, *9*, 661–674. [[CrossRef](#)]
74. Dăscălescu, D.; Apetrei, C. Nanomaterials Based Electrochemical Sensors for Serotonin Detection: A Review. *Chemosensors* **2021**, *9*, 14. [[CrossRef](#)]
75. Apetrei, R.M.; Cârâc, G.; Bahrim, G.; Camurlu, P. Sensitivity Enhancement for Microbial Biosensors through Cell Self-Coating with Polypyrrole. *Int. J. Polym. Mater. Polym. Biomater.* **2019**, *68*, 1058–1067. [[CrossRef](#)]
76. Bounegru, A.V.; Apetrei, C. Development of a Novel Electrochemical Biosensor Based on Carbon Nanofibers–Gold Nanoparticles–Tyrosinase for the Detection of Ferulic Acid in Cosmetics. *Sensors* **2020**, *20*, 6724. [[CrossRef](#)] [[PubMed](#)]
77. Bounegru, A.V.; Apetrei, C. Simultaneous Determination of Caffeic Acid and Ferulic Acid Using a Carbon Nanofiber-Based Screen-Printed Sensor. *Sensors* **2022**, *22*, 4689. [[CrossRef](#)] [[PubMed](#)]
78. Rand, E.; Periyakaruppan, A.; Tanaka, Z.; Zhang, D.A.; Marsh, M.P.; Andrews, R.J.; Lee, K.H.; Chen, B.; Meyyappan, M.; Koehne, J.E. A Carbon Nanofiber Based Biosensor for Simultaneous Detection of Dopamine and Serotonin in the Presence of Ascorbic acid. *Biosens. Bioelectron.* **2013**, *42*, 434–438. [[CrossRef](#)]
79. Fayemi, O.E.; Adekunle, A.S.; Ebenso, E.E. Electrochemical Determination of Serotonin in Urine Samples Based on Metal Oxide Nanoparticles/MWCNT on Modified Glassy Carbon Electrode. *Sens. Bio-Sens. Res.* **2017**, *13*, 17–27. [[CrossRef](#)]
80. Ran, G.; Chen, X.; Xia, Y. Electrochemical Detection of Serotonin Based on a Poly(Bromocresol Green) Film and Fe₃O₄ Nanoparticles in a Chitosan Matrix. *RSC Adv.* **2017**, *7*, 1847–1851. [[CrossRef](#)]
81. Satyanarayana, M.; Koteswara Reddy, K.; Vengatajalabathy Gobi, K. Nanobiocomposite Based Electrochemical Sensor for Sensitive Determination of Serotonin in Presence of Dopamine, Ascorbic Acid and Uric Acid In Vitro. *Electroanalysis* **2014**, *26*, 2365–2372. [[CrossRef](#)]
82. Dinesh, B.; Veeramani, V.; Chen, S.M.; Saraswathi, R. In Situ Electrochemical Synthesis of Reduced Graphene Oxide–Cobalt Oxide Nanocomposite Modified Electrode for Selective Sensing of Depression Biomarker in the Presence of Ascorbic Acid and Dopamine. *J. Electroanal. Chem.* **2017**, *786*, 169–176. [[CrossRef](#)]

83. Dăscălescu, D.; Apetrei, C. Voltammetric Determination of Levodopa Using Mesoporous Carbon—Modified Screen-Printed Carbon Sensors. *Sensors* **2021**, *21*, 6301. [[CrossRef](#)]
84. Application of Fourier Transform Infrared (FTIR) Spectroscopy Coupled with Multivariate Calibration for Quantitative Analysis of Curcuminoid in Tablet Dosage Form. *J. Appl. Pharm. Sci.* **2018**, *8*, 151–156. [[CrossRef](#)]
85. Bel'skaya, L.V.; Sarf, E.A.; Solomatin, D.V. Application of FTIR Spectroscopy for Quantitative Analysis of Blood Serum: A Preliminary Study. *Diagnostics* **2021**, *11*, 2391. [[CrossRef](#)] [[PubMed](#)]